UNIVERSIDAD CARLOS III DE MADRID working papers

UC3M Working Papers
Statistics and Econometrics
15-07
ISSN 2387-0303
May 2015

Departamento de Estadística
Universidad Carlos III de Madrid
Calle Madrid, 126
28903 Getafe (Spain)
Fax (34) 91 624-98-48

Adaptive EWMA Control Charts with a Time Varying Smoothing Parameter

Willy Ugaz[a,*], Ismael Sánchez[a]

Abstract

It is known that time-weighted charts like EWMA or CUSUM are designed to be optimal to detect a specific shift. If they are designed to detect, for instance, a very small shift, they can be inefficient to detect moderate or large shifts. In the literature, several alternatives have been proposed to circumvent this limitation, like the use of control charts with variable parameters or adaptive control charts. This paper has as main goal to propose some adaptive EWMA control charts (AEWMA) based on the assessment of a potential misadjustment, which is translated into a time-varying smoothing parameter. The resulting control charts can be seen as a smooth combination between Shewhart and EWMA control charts that can be efficient for a wide range of shifts. Markov chain procedures are established to analyze and design the proposed charts. Comparisons with other adaptive and traditional control charts show the advantages of the proposals.

Keywords:

Adaptive control charts, Average Run Length, EWMA, Statistical Process Control.

[a] Department of Statistics, Universidad Carlos III de Madrid.
[a,*] Corresponding autor.

Acknowledgements: financial support from the Spanish Ministry of Education and Science, research project ECO2012-38442.

Adaptive EWMA Control Charts with a Time Varying Smoothing Parameter

Willy Ugaz and Ismael Sánchez*

Universidad Carlos III de Madrid

May 8, 2015

Abstract

It is known that time-weighted charts like EWMA or CUSUM are designed to be optimal to detect a specific shift. If they are designed to detect, for instance, a very small shift, they can be inefficient to detect moderate or large shifts. In the literature, several alternatives have been proposed to circumvent this limitation, like the use of control charts with variable parameters or adaptive control charts. This paper has as main goal to propose some adaptive EWMA control charts (AEWMA) based on the assessment of a potential misadjustment, which is translated into a time-varying smoothing parameter. The resulting control charts can be seen as a smooth combination between Shewhart and EWMA control charts that can be efficient for a wide range of shifts. Markov chain procedures are established to analyze and design the proposed charts. Comparisons with other adaptive and traditional control charts show the advantages of the proposals.

Keywords: Adaptive control charts, Average Run Length , EWMA, Statistical Process Control.

* *Address:* Willy Ugaz and Ismael Sánchez, Departamento de Estadística; Universidad Carlos III de Madrid; Avd. de la Universidad 30, 28911, Leganés, Madrid (Spain). email: wugaz@est-econ.uc3m.es, ismael@est-econ.uc3m.es.

1 Introduction

The research published by Walter Shewhart (1931) about the fundamentals of SPC (Statistical Process Control) supposed a change of paradigm in the concept of quality control, because it changed the focus from a control based on the verification of the final specifications to a control based on the monitoring of the intrinsic variability of a process. Shewhart proposed charts based on monitoring the value of a statistic on independent samples, usually denoted as rational subgroups. These charts are known as Shewhart Control Chart. Let X be a random variable representing a quality characteristic of a product obtained from the process we want to monitor. Let us denote the mean and variance of X when the process is in control as μ_0 and σ^2, respectively. Let $x_{i1}, x_{i2}, ..., x_{in}$ be a set of realizations of X which conform the i-th rational subgroup of size n, being $\bar{x}_i$ its sample mean. A Shewhart $\bar{X}$ control chart monitors the evolution of the sequence of the independent sampling means $\bar{x}_i$ with the aim of controlling that the process mean has not changed. Under the assumption that $\bar{X}$ is normal, the control limits of the Shewhart $\bar{X}$ chart are

$$\mu_0 \pm 3\sigma/\sqrt{n}. \tag{1}$$

These limits represent a probability interval of $\bar{X}$ of coverage $1 - \alpha = 0.9973$. The chart triggers an alarm if a sample mean falls outside these limits. The probability of a false alarm is then $\alpha = 0.0027$. Similarly, there are Shewhart control charts for some other statistics, like sampling variances, standard deviations, coefficient of variations and so forth.

It is well known that $\bar{X}$ control charts and, in general, Shewhart charts, are not very sensitive to small shifts in the process mean. For example, it is easy to find out that if the shifted mean μ_1 is such that $|\mu_1 - \mu_0| < 2\sigma$, the probability of detecting such change with the chart (1) is very small for practical purposes. In order to detect small shifts we need a statistics with lower variance that, for a given false alarm rate, can provide narrower control limits. This could be attained with a larger subgroup size n. However, since Shewhart charts are based on independent samples, a larger rational subgroup size might lead to a larger average time to signal (ATS), or a larger average number of observations to signal (ANOS).

In order to increase the sensitivity of Shewhart control charts to smaller shifts, the literature have proposed some modifications, such as the use of supplementary run rules. The run rules are a set of rules that help to detect when a sequence of several points (run) in a Shewhart chart is very unlikely when the process is in control, showing evidence of misadjustment. An unlikely run will trigger an alarm even if the points are inside the control limits. Consequently, the shift does not need to surpass the control limits to be detected. Runs Rules for Shewhart charts have been proposed,

among others, by Page (1955a), Western Electric (1956), Reynolds (1971), Nelson (1984), Champ and Woodall (1987), Davis and Woodall (1988), Davis et al. (1990), Derman and Ross (1997), Klein (2000), Khoo and Ariffin (2006), Acosta-Mejía (2007), Koutras et al. (2007), and Antzoulakos and Rakitzis (2008).

Another proposal to improve the sensitivity of Shewhart control charts to small shifts is by means of an adaptive design of its parameters; typically, variable sample sizes (VSS), variable sampling intervals (VSI) or some combination of both approaches. The main idea of this approach is to increase the sampling (size or frequency) only when data show some evidence of a shift. By doing so, we could take advantage of the larger information without incurring in a high cost. Basically, in a VSS chart, if the point falls in the warning region, i.e. a region inside the control limits but close to them, the next sample size should be large to increase the sensitivity of the chart. However, if the point falls in the central region, the next sample size can be small, since there is no evidence that the process had shifted (see Daudin, 1992; Prabhu et al., 1993, 1994; Costa, 1994; Zimmer et al., 1998; and, more recently, Wu, 2011; Zhang and Wang, 2012, and Castagliola et al., 2012). Similarly, in a VSI chart, the time to take the next sample should be smaller if the point falls in the warning region because the process could need a quick adjustment. Conversely, the time to take the next sample can be large if the current point falls in the central region, since the risk of being out of control is very low (see Reynolds et al.,1988; Cui and Reynolds, 1988; Runger and Pignatiello, 1991; Costa, 1994, 1999a, 1999b; Tagaras, 1998; Mahadik, 2013).

An alternative procedure to reduce the variance of the monitoring statistics is to use a statistic with memory; that is, a statistics based on some average of current and past data, instead of a statistics based on independent samples. By doing so, we are increasing the effective sample size, leading to a reduction in the sampling variability that would ease the detection. By using a chart with memory, we are not increasing the sampling costs. However, merging present and past observations in the same statistics can have a negative effect. If the process mean shifts, a monitoring statistics with memory would merge data corresponding to the shifted process with previous data when the process was in control. This effect would bias the value of the statistics, masking the shift. This can also provoke a delay in the detection. Therefore, if the shift is large, it might not be worthwhile to use a monitoring statistics with memory. Hence, this kind of charts, denoted as memory charts or time-weighted charts, are then useful only in the case of small shifts. The decision of whether to use a Shewhart control chart or a memory control chart can then be interpreted as a particular case of the traditional bias-variance trade-off. The most popular memory charts are the CUSUM and the EWMA charts. CUSUM control charts were introduced by Page (1954, 1955b) and then studied, among others, by Woodall and Adams

(1993).

Charts with memory can be applied to monitor the information of rational subgroups; however, they are frequently used for individual observations. Let x_t, $t = 1, 2, ...$, be a sequence of independent realizations of the random variable X that, when the process is in control, holds $X \sim N(\mu_0, \sigma^2)$. The CUSUM chart, which in fact is a two-side chart, uses two different statistics, C_t^+ and C_t^-, that monitor the cumulative sum of positive and negative deviations from μ_0, respectively, as

$$C_t^+ = \max\left[0, C_{t-1}^+ + (X_t - \mu_0) - K\right], \tag{2a}$$

$$C_t^- = \max\left[0, C_{t-1}^- - (X_t - \mu_0) - K\right], \tag{2b}$$

with $C_0^+ = C_0^- = 0$. If the accumulated deviation is larger than K, (in absolute value) then the statistics C_t^+ or C_t^- will increase the memory of the chart, otherwise they are reset to 0. A small value of K will facilitate a larger memory, and, consequently a smaller variance of the statistics. Consequently, smaller shifts can be detected. By means of K, the CUSUM chart can be designed to detect shifts of a specific size, usually expressed in terms of the standard deviation as $\mu_1 = \mu_0 + \delta\sigma$. Then, K is defined as $K = k\sigma$, with $k = |\delta|/2$. Then the parameter k rules the memory of this chart. A low value of k would increase the memory, which is needed to detect small shifts. Conversely, a large value of k will only be surpassed by large deviations. When C_t^+ or C_t^- exceed a threshold value H, the process is considered out of control. The H parameter is also defined according to the standard deviation as $H = h\sigma$. The optimal value of h to attain a desired Average Run length (ARL) when the process is in control, denoted as ARL_0, depends on the sensitivity parameter k (Vance, 1986; Hawkins, 1992, 1993).

The EWMA control chart proposes a different procedure to weight historical information. It was introduced by Roberts (1959) and subsequently studied by Robinson and Ho (1978), Hunter (1986), Waldmann (1986), Montgomery, Gardiner and Pizzano (1987), Crowder (1987a and 1989) and Lucas and Saccucci (1990), among others. Its statistic is defined as

$$y_t = \lambda x_t + (1 - \lambda)\, y_{t-1}, \tag{3}$$

where $\lambda \in (0, 1]$. If $\lambda < 1$, the statistics (3) is a weighted average of current and past observations. The smaller the λ the larger the weight to past data and, hence, the larger the effective sample size. Therefore, if we want to detect a small shift we would use a small value of λ. The variance of y_t for a large values of t converges to

$$\sigma_{y_t}^2 = \sigma^2 \frac{\lambda}{2 - \lambda}, \tag{4}$$

that can be interpreted as that, at the long term, the EWMA chart averages an equivalent number of observations of $M = (2 - \lambda)/\lambda$, that increases as λ diminishes. The eventual control limits of the

EWMA chart are then

$$\mu_0 \pm L\sigma\sqrt{\frac{\lambda}{2-\lambda}}, \tag{5}$$

where L is a parameter that depends on the desired ARL_0. Also, with the aim of improving their performance, VSL and VSS CUSUM and EWMA control charts have been proposed by Sawalapurkar et al. (1990), Reynolds et al. (1990), Baxley (1995), Keats et al. (1995), Reynolds (1995, 1996), Stoumbos and Reynolds (1996, 1997), Reynolds and Stoumbos (1998), Reynolds and Arnolds (2001), Arnolds and Reynolds (2001) and Tagaras (1998), among others.

Alternatively, adaptive CUSUM and EWMA charts can be proposed based on time-varying versions of the parameters that control the memory of the charts; that is k in CUSUM charts and λ in EWMA charts. By adapting the memory, we can make the charts sensitive both to small and large shifts. The intuition behind these adaptive charts is to use a measure of the potential presence of a shift. Accordingly, the value of their parameter is increased when it is suspected that the process could be out of control due to a large shift. Conversely, if the data show large evidence of being in control or with a small shift, the parameters tend to be smaller, easing the detection of potential small shifts. This kind of adaptation scheme is the one we are interested in this article.

Sparks (2000) developed adaptive CUSUM (ACUSUM) charts to detect unknown shifts. The procedure is based on estimating the size of the potential shift, $\hat{\delta}$, using a simple exponentially weighted moving average and doing one-step-ahead forecasts. Then, the ACUSUM is build using $k = |\hat{\delta}|/2$ and appropriate control limits. Jiang et al. (2008) improves the chart of Sparks (2000) by applying likelihood ratio testing concepts in the estimation of the potential shift. Other contributions for ACUSUM charts can be found, among others, in Shu and Jiang (2006), Han et al. (2007) and Shu et al. (2008).

Capizzi and Masarotto (2003) developed an adaptive EWMA chart (AEWMA) based on weighting recent observations using an appropriate function of the current error $e_t = x_t - y_{t-1}$. The goal of this weighting scheme is to diminish the so-called inertia problem of the EWMA charts (Yashchin, 1987), that reduces the efficiency of the detection. The resulting AEWMA chart produces a time varying smoothing parameter λ according to the evolution of the process. In particular, if e_t is small, the value of λ tends to be small, like in conventional EWMA chart, since the process seems to be in control. However, if e_t is large the value of λ tends to be large, since the risk of being out of control is higher. Other research of interest to study adaptive EWMA charts can be found in Steiner (1999), Hang y Tsung (2004), Costa and Rahim (2006), and Shu (2008).

In this article, alternative AEWMA charts are proposed. To that aim, several measures of the potential shift of the process are suggested, being the proposal of Capizzi and Masarotto (2003) a

particular case. For each measure of potential shift, alternative methods to translate such measure into a time varying smoothing factor are discussed. Procedures to compute the ARL and optimize the charts based on Markov chain approximations are proposed. A numerical comparison of these alternative approaches and the main alternatives in the literature is presented.

The rest of the article is organized as follows. In Section 2 the notion of the adaptive EWMA control chart is introduced. In Section 3 AEWMA control charts with time varying λ_t based on the last observation are proposed. In Section 4 AEWMA control charts with time varying λ_t based on the level of the control statistics are proposed. Section 5 proposes several comparisons between alternative control charts and the proposed AEWMA control charts. Finally, in Section 6 some concluding remarks are given.

2 Adaptive EWMA control chart

The design of an EWMA chart consist of selecting the values of λ in (3) and L in (5). They can be chosen in such a way that the chart is optimal for detecting a prespecified shift for a given ARL_0. The influence of the design parameters in the performance of the EWMA has been studied by Crowder (1987a, 1989) and Lucas and Saccucci (1990) among others. They can be based on approximating the ARL with a discrete Markov chain. The resulting ARL is then a function of δ, λ and L; that is, ARL$\equiv$ARL(δ, λ, L). For a prespecified shift $\delta\sigma$, it can be written as ARL_δ =ARL$(\lambda, L|\delta)$. Then, the optimal values of λ and L that minimize ARL$(\lambda, L|\delta)$ can be obtained using traditional nonlinear optimization procedures. This optimization problem can be written as

$$\begin{aligned} &\min\left(ARL\left(\lambda, L|\delta\right)\right), \\ &\text{subject to:} \\ &ARL\left(\lambda, L|\delta = 0\right) = ARL_0. \end{aligned}$$

We have calculated the optimal design for each shift and $\text{ARL}_0 = 100$. The minimum ARL is denoted by ARL^*. Figure 1-a shows the comparison between the optimal design for ARL^* and the range of designs with $ARL \leq ARL^* + 5\%$. That is, we find the optimal design for each shift as well as those designs that are nearly optimal in the sense that their ARL in each shift is not larger than a 5% of the minimum one. Table 1 shows that, for instance, if $\delta = 1$ then it is possible to get an $ARL \in [6.96, 7.31]$ for a $\lambda \in [0.0874, 0.3158]$. The Figure (1-b) shows the range (λ_1, λ_2) of λ for which the value of ARL varies in the range $(ARL^*, ARL^* + 5\%)$. For example, if $\lambda = 0.15$, it possible to get acceptable values of ARL (with a difference lower than 5% of ARL^*) for small shifts from $\delta \approx 0.75$ to 1.25. If $\lambda = 0.6$, it is possible to get acceptable values of ARL for $\delta > 2$. However, we see that if we want an EWMA with a good performance for all shifts, we need to change the value of λ.

δ	**Optimal** λ	**ARL***	**ARL*****+5%**	$(\lambda_1 - \lambda_2)$
0.10	0.0100	75.71	79.50	(0.0100-0.0800)
0.25	0.0238	38.11	40.01	(0.0100-0.0734)
0.50	0.0664	17.33	18.20	(0.0210-0.1408)
0.75	0.1211	10.28	10.79	(0.0514-0.2252)
1.00	0.1830	6.96	7.31	(0.0874-0.3158)
1.25	0.2501	5.11	5.36	(0.1278-0.4101)
1.50	0.3235	3.95	4.15	(0.1725-0.5082)
1.75	0.4051	3.18	3.34	(0.2241-0.6086)
2.00	0.4926	2.62	2.75	(0.2861-0.7070)
2.25	0.5789	2.21	2.32	(0.3559-0.7994)
2.50	0.6580	1.89	1.98	(0.4235-0.8842)
2.75	0.7276	1.64	1.72	(0.4808-0.9625)
3.00	0.7876	1.45	1.53	(0.5235-1.0000)
3.25	0.8384	1.31	1.38	(0.5994-1.0000)
3.50	0.8807	1.21	1.27	(0.5576-1.0000)
3.75	0.9150	1.13	1.19	(0.5467-1.0000)
4.00	0.9421	1.08	1.14	(0.5175-1.0000)
4.25	0.9625	1.05	1.10	(0.4726-1.0000)
4.50	0.9771	1.03	1.08	(0.4171-1.0000)
4.75	0.9869	1.02	1.07	(0.3579-1.0000)
5.00	0.9930	1.01	1.06	(0.3015-1.0000)

Table 1: Minimum ARL for each shift $\delta\sigma$ and the corresponding λ .

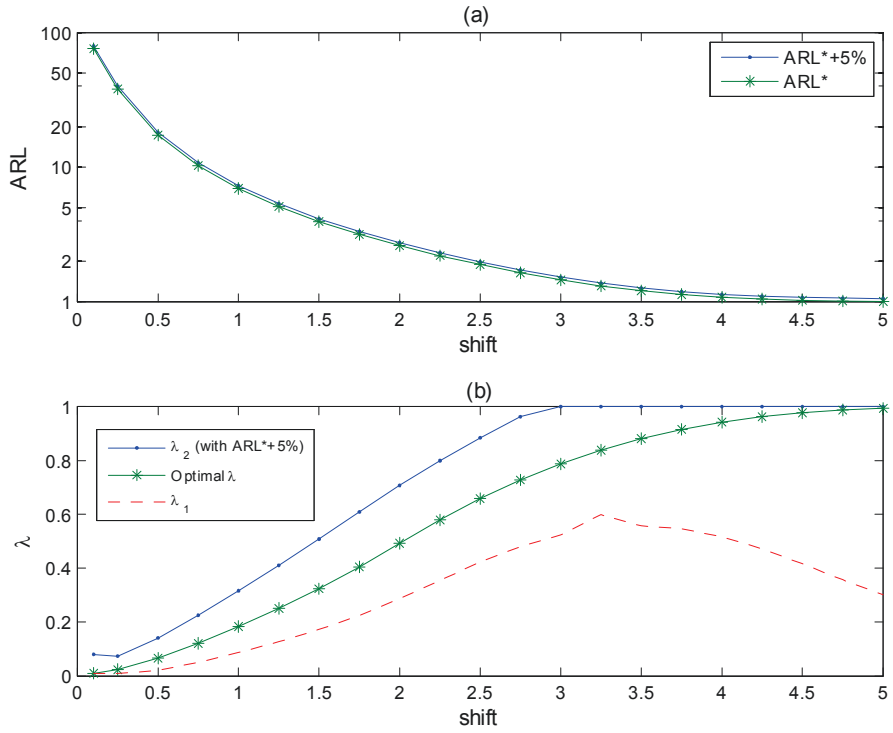

Figure 1: (a) Comparison between the ARL^* (-$*$-) and $ARL^* + 5\%$ (-··-). (b) the optimal λ behavior (-$*$-), and a range of variation defined by λ_1 (- -) and λ_2 (-··-).

The goal of an AEWMA charts is to have a performance that is optimal or nearly optimal for any shift. This could be attained by making λ time-varying, that is $\lambda = \lambda_t$, with a value that is dependent on the shift, as shown above. However, in practice, the shift is unknown (otherwise, we would trigger the alarm). Therefore it is necessary to find an alternative way to make an EWMA chart adaptive. A natural option is to find a measure of the evidence of shift shown by the data, and translate that measure in an appropriate value λ_t. If data suggest that the process mean could be shifting, the value of λ_t would increase to allow y_t to get rid of the old information, and get closer to the new mean, which, in turn, will ease to trigger the alarm. Conversely, if data show low evidence of being shifting, the parameter λ_t would be kept at a lower value, to allow the detection of a possible small shift. In the literature, the only proposal for AEWMA chart based on the behavior of data is Capizzi and Masarotto (2003), which consider the statistic

$$y_t = y_{t-1} + \phi\left(e_t\right); \quad y_0 = \mu_0, \tag{6}$$

where $e_t = x_t - y_{t-1}$, and $\phi\left(e_t\right)$ is a score function that depends on e_t. A signal of upward or downward shift is issued when $|y_t - \mu_0| > h\sigma$, where h is a threshold that determines the ARL_0. When $x_t \neq y_{t-1}$,

(6) could be rewritten as

$$y_t = w(e_t)\, x_t + (1 - w(e_t))\, y_{t-1},$$

i. e., it is an EWMA statistic with variable weights because $w(e) = \phi(e)/e$. $\phi(e)$ should be monotonically increasing in e; $\phi(e) = -\phi(-e)$; $\phi(e) \approx \lambda e$, when $|e|$ is small, for a suitable λ, $0 < \lambda \leq 1$; and finally $(e)/e \approx 1$, when the $|e|$ value is large. Capizzi and Masarotto (2003) proposes the following score function, based on the Huber function:

$$\phi_{hu}(e) = \begin{cases} e + (1-\lambda)\, k & \text{si } e < -k \\ \lambda e & \text{si } |e| \leq k \\ e - (1-\lambda)\, k & \text{si } e > k \end{cases}, \tag{7}$$

where, if $k \to \infty$, then $\phi_{hu}(e) = \lambda e$ and the AEWMA chart reduces to the traditional EWMA (3). Moreover, when $\lambda = 1$ or $k = 0$, the AEWMA chart performs essentially like a Shewhart chart. This AEWMA chart can be interpreted as a chart with a time varying smoothing parameter $w(e_t)$ according to the process data. In particular, if the current observation is close to the previous value of the EWMA statistic, then the value of $w(e_t)$ must be small (conventional EWMA chart), but if the current observation is not near the previous value of the EWMA statistic, then the value of $w(e_t)$ should be large, in that case EWMA chart will be similar to Shewhart chart (see Shewhart, 1931).

In this work we will analyze alternative strategies to get AEWMA charts with time-varying smoothing parameters, using the representation

$$y_t = \lambda_t x_t + (1 - \lambda_t)\, y_{t-1}, \quad y_0 = \mu_0, \tag{8}$$

and where the proposal of Capizzi and Masarotto (2003) is a particular case. The alarm is triggered as soon as $|y_t - \mu_0| > h\sigma$, where h is a threshold that determines the ARL_0. In each case, a specific statistics that quantify the evidence of a shift from data is proposed. Then, a Markov chain representation is obtained to compute the ARL. This Markov chain representation is used to optimize the parameters such that minimum ATL is attained for a given ARL_0.

3 AEWMA charts with λ_t based on the last observation x_t

In this section, we present some proposals for λ_t as a function of the potential misadjustment based on the information provided by the last observation x_t. The first proposal, denoted as AEWMA1, is based on the standardized distance from x_t and the target μ_0. The second proposal, denoted as AEWMA2, is based on the standardized distance form x_t and the last value of the monitoring statistics y_{t-1}. Alternative ways of translating each distance into a smoothing factor λ_t are proposed. The AEWMA chart of Capizzi and Massaroto (2003) can be interpreted as a particular case of this second distance.

3.1 The AEWMA1 chart

This adaptive control chart measures the potential missadjustment by standardizing the last observation x_t. This is done by using the following statistics:

$$S_{1t} = \left(\frac{x_t - \mu_0}{\sigma} \right)^2, \tag{9}$$

which is a measure of the actual distance of the process to the target. This distance will tend to be larger in presence of a shift, therefore it is an interesting measure of the potential misadjustment. Given y_{t-1}, the value of x_t is a random variable. If the process is in control, and under the assumption of normality, it holds that $S_{1t} \sim \chi^2_1$, with a cumulative distribution function defined as

$$F_{1t} = P\left(\chi^2_1 \leq S_{1t}\right). \tag{10}$$

Note that $F_{1t} \in [0, 1]$ and, besides, it tends to approach unity as the process departures from the in-control state. Therefore, it could be used as λ_t. However, the variability of F_{1t} can be very large, provoking a poor performance in the AEWMA chart. It should be noted that, according to (8), a large value of λ_t implies the lost of most of the memory accumulated in y_{t-1}, and that can no longer be recovered even if λ_t decreases in the following instants. This lost of memory would lead to a large variance of the monitoring statistics y_t, decreasing its sensitivity. We need, then, some efficient transformation that helps to translate F_{1t} into a smoothing parameter λ_t. Many transformations can be proposed. A simple transformation would be to limit the range of variation of F_{1t}, doing a linear transformation between some lower value $\lambda_{\min}$ and an upper value $\lambda_{\max}$ as follows:

$$\lambda^{(1)}_{1t} = \lambda_{\min} + (\lambda_{\max} - \lambda_{\min}) F_{1t}, \tag{11}$$

where $\lambda_{\min}$ and $\lambda_{\max}$ are values that are optimized to attain the lowest ARL for a given ARL_0, and computed with a procedure described below. A second alternative that adds some flexibility to the transformation (11) is to also use a power transformation as

$$\lambda^{(2)}_{1t} = \lambda_{\min} + (\lambda_{\max} - \lambda_{\min}) F^a_{1t}, \tag{12}$$

where a is can also optimized together with $\lambda_{\min}$ and $\lambda_{\max}$. The third proposal to transform F_{1t} into λ_t is to use some threshold value, p_0, such that if $F_{1t} \leq p_0$ then $\lambda_t = \lambda_{\min}$. Consequently, we will maintain a low smoothing factor unless the evidence of shift is large. If $F_{1t} > p_0$, we maintain a similar transformation as in (12) in such a way that the whole transformation is continuous. The resulting

smoothing factor is

$$\begin{aligned} \lambda_{1t}^{(3)} &= \lambda_{\min} + (\lambda_{\max} - \lambda_{\min})\, q_{1t}, \\ q_{1t} &= \begin{cases} 0 & \text{if } F_{1t}^{a} \leq p_0, \\ \dfrac{F_{1t}^{a} - p_0}{1 - p_0} & \text{otherwise,} \end{cases} \end{aligned} \tag{13}$$

where the percentile p_0 is also a constant to be optimized together with c, $\lambda_{\min}$, and $\lambda_{\max}$. A fourth alternative with further flexibility is to fit the following polynomial:

$$\lambda_{1t}^{(4)} = \max(0, \min(1, r_{1t})), \tag{14}$$

$$r_{1t} = d + (b + cF_{1t})^{a}. \tag{15}$$

This fourth option, needs also the optimization of four parameters. In our experiments, the option (13) has been the one with better performance. Therefore, for the sake of conciseness, this transformation will be the only one that will be assumed in this work for the proposed AEWMA charts. Figure 2 shows two examples of how the value x_t is translated into a smoothing factor λ_t, with $\lambda_t = \lambda_{1t}^{(3)}$ in (13) for alternative values of $a, p_0, \lambda_{\min}$, and $\lambda_{\max}$.

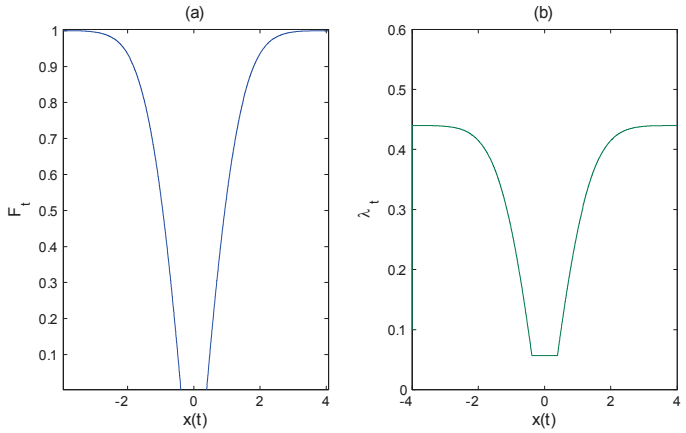

Figure 2: (a) Behavior of F_t in terms of x_t. (b) Behavior of λ_t parameter in terms of behavior x_t. To obtain these curves, a specific AEWMA1 chart design has been considered.

3.2 The AEWMA2 chart

This adaptive control chart measures the potential misadjustment by controlling the difference between the current observation x_t and the value of the AEWMA statistic in the previous time, y_{t-1}. This is done by using the following statistics

$$S_{2t} = \left(\frac{x_t - y_{t-1}}{\sigma} \right)^2, \tag{16}$$

that similarly to the previous proposal, tends to increase in presence of a shift. This statistics holds that

$$S_{2t} = \left(\frac{x_t - \mu_0}{\sigma} + \frac{\mu_0 - y_{t-1}}{\sigma} \right)^2 = \left(z_t + \frac{\mu_0 - y_{t-1}}{\sigma} \right)^2, \tag{17}$$

where $z_t \sim N(0,1)$. Then, conditioning on y_{t-1}, S_{2t} follows a non-central chi-square distribution of one degree of freedom, $\chi^2_1(\gamma_t)$, with noncentrality parameter $\gamma_t = (\mu_0 - y_{t-1})/\sigma$. The cumulative distribution function is then

$$F_{2t} = P(\chi^2_1(\gamma_t) \leq S_{2t}), \tag{18}$$

as in the AEWMA1 chart, we could use F_{2t} to translate S_{2t} into a smoothing parameter, and the transformation (12) to obtain a time-varying smoothing parameter. It can be seen, however, that the noncentrality parameter γ_t can be very small. For instance, if $\lambda = 0.1$, expression (4) shows that $\sigma^2_{y_t} \approx 0.1\sigma^2$. Therefore, since $E(y_t) = \mu_0$, the noncentrality parameter can be neglected for practical purposes. Therefore, for the sake of simplicity, the conversion of S_{2t} into a smoothing factor will be done as

$$\begin{aligned} \lambda_{2t} &= \lambda_{\min} + (\lambda_{\max} - \lambda_{\min})\, q_{2t}, \\ q_{2t} &= \begin{cases} 0 & \text{if } G^a_{2t} \leq p_0, \\ \dfrac{G^a_{2t} - p_0}{1 - p_0} & \text{otherwise,} \end{cases} \\ G_{2t} &= P(\chi^2_1 \leq S_{2t}). \end{aligned} \tag{19}$$

where the parameters $\lambda_{\min}$, $\lambda_{\max}$, p_0, and a, are optimized to minimize the ARL when the process is out of control, for a given ARL_0 using the procedure shown below. Figure 3 illustrates how λ_{2t} varies as a function of x_t, with two particular combination of parameters. Since the statistics S_{2t} depends on y_{t-1} two curves with different values of y_{t-1} are displayed. When $y_{t-1} = 0$, the method is similar to the AEWMA1.

3.3 The AEWMA3 chart

This chart is a combination of the AEWMA1 and AEWMA2 charts. In order to speed up adaptation, this chart behaves like the AEWMA1 or the AEWMA2, depending on which statistics, S_{1t} or S_{2t}, is more pessimistic with respect to the evidence of misadjustment. With this aim, the AEWMA3 chart uses the following time-varying smoothing factor:

$$\lambda_{3t} = \max(\lambda^{(2)}_{1t}, \lambda_{2t}) \tag{20}$$

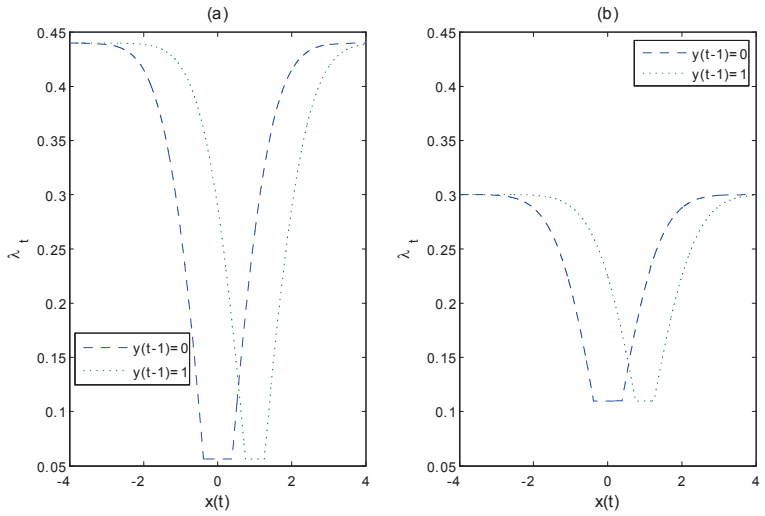

Figure 3: (a) Behavior of λ_t parameter in terms of x_t with $y_{t-1} = 0$ $(--)$ and $y_{t-1} = 1$ $(\cdots)$ for a specific AEWMA2 control chart design. (b) Behavior of λ_t parameter in terms of behavior x_t with $y_{t-1} = 0$ $(--)$ and $y_{t-1} = 1$ $(\cdots)$ for a specific AEMWA 2 control chart design.

3.4 Computation of the ARL of using a Markov chain approach

This section shows a procedure to compute the ARL of the AEWMA1, AEWMA2, and AEWMA3 charts using a Markov chain approach. Similarly to the Markov chain model suggested by Lucas y Saccucci (1990) or Capizzi and Masarotto (2003), we can approximate the value of ARL by discretizing the infinite-state transition probability matrix of the continuous-state Markov chain defined by (8). For convenience, we rewrite the control statistics of the AEWMA as

$$y_t = y_{t-1} + (x_t - y_{t-1})\,\lambda_t. \tag{21}$$

The procedure consists in dividing the interval defined by the upper and the lower control limits, of width $2h\sigma$, in an odd number $ms = 2m+1$ of subintervals Ω_j, $j = -ms, -ms+1, ..., ms$, of width $\delta = 2h\sigma/ms$. The intervals Ω_j are then interpreted as states. The control statistic y_t is considered to be in the transient state Ω_j, at time t, if $\nu_j - \delta/2 < y_t < \nu_j + \delta/2$, where ν_j is the midpoint of the jth interval Ω_j. Furthermore, y_t falls in an absorbing state when it exceeds a threshold $H = \mu_0 + h\sigma$ or $-H$. The transition probability matrix between states can be represented in partitioned form as

$$\mathbf{P} = \begin{pmatrix} \mathbf{R} & (\mathbf{I} - \mathbf{R})\,\mathbf{u} \\ \mathbf{0} & 1 \end{pmatrix}, \tag{22}$$

where $\mathbf{R}$ is a $ms \times ms$ submatrix that contains the probabilities p_{jk} of going from the transient state j to the state k, $\mathbf{I}$ is the $ms \times ms$ identity matrix, and $\mathbf{u}$ is a $ms \times 1$ vector of ones. The elements of the

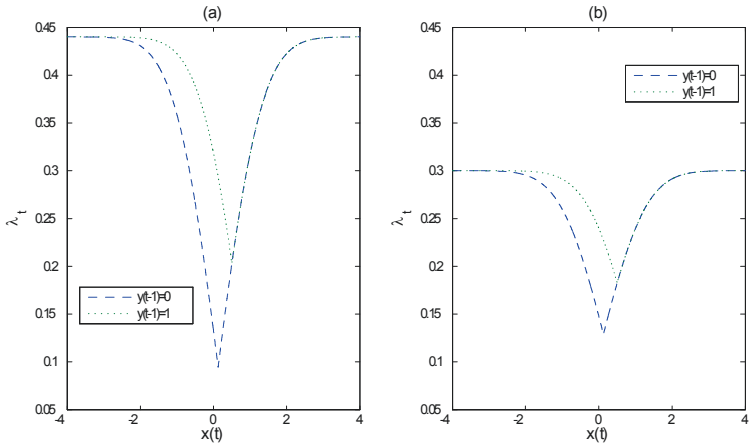

Figure 4: (a) Behavior of λ_t parameter in terms of x_t with $y_{t-1} = 0$ $(--)$ and $y_{t-1} = 1$ $(\cdots)$ for a specific AEWMA3 control chart design. (b) Behavior of λ_t parameter in terms of behavior x_t with $y_{t-1} = 0$ $(--)$ and $y_{t-1} = 1$ $(\cdots)$ for a specific AEMWA 3 control chart design.

vector $(\mathbf{I} - \mathbf{R})\,\mathbf{u}$ are the probabilities of jumping to the absorbing state from state j. To approximate these probabilities, it is customary to assume that the statistic y_{t-1} is equal to ν_j whenever it is in state j. Using the form in (21), this produces

$$\begin{aligned} r_{jk} &= \Pr\left(y_t \in \Omega_k |\ y_{t-1} \in \Omega_j\right) \\ &= \Pr(\nu_k - \delta/2 < y_t \leq \nu_k + \delta/2 |\ y_{t-1} = v_j) \qquad (23) \\ &= \Pr\left\{\nu_k - \delta/2 < \nu_j + (x_t - \nu_j)\,\lambda_t \leq \nu_k + \delta/2\right\}, \\ &= \Pr\left\{\nu_k - \nu_j - \delta/2 < (x_t - \nu_j)\,\lambda_t \leq \nu_k - \nu_j + \delta/2\right\}. \qquad (24) \end{aligned}$$

Since λ_t depends on x_t (e.g., (13)), we can not solve for x_t in (24), and it is not trivial how the product $(x_t - \nu_j)\,\lambda_t$ is distributed. Therefore, in order to estimate that distribution, we discretize x_t in $nx = 2n + 1$ subintervals ψ_i, $i = -n, -n+1, ..., n$. Since $x_t \sim N(\mu, \sigma^2)$, we first select an interval of very high probability, and divide it into subintervals. Accordingly, we divide the interval $\mu \pm 4.5\sigma$, into $2n - 1$ subintervals ψ_i, $i = -n+1, -n+2, ..., n-1$, of width $\varepsilon = 9\sigma/2n$, being u_i the midpoint of the ith subinterval ψ_i. If $x_t \in \psi_i$ then $u_i - \varepsilon/2 < x_t \leq u_i + \varepsilon/2$. In each of these subintervals, we approximate x_t to the value u_i. We have then two more subintervals, which are at the tails the distribution of x_t. The lower tail is the interval ψ_{-n}. If $x_t \in \psi_{-n}$ then $x_t \leq u_{-n+1} - \varepsilon/2$, and would approximate x_t to the value $u_{-n+1} - \varepsilon$. Similarly, the upper tail is the interval ψ_n. If $x_t \in \psi_n$ then $x_t > u_{n-1} + \varepsilon/2$, and would approximate x_t to the value $u_{n-1} + \varepsilon$. The approximate values for x_t can

be used to assign an approximate value to λ_t in each subinterval. If $x_t \in \psi_i$, then

$$\begin{aligned} S_{1t} &\approx \left(\frac{u_i-\mu_0}{\sigma}\right)^2 \equiv e_i \text{ or } S_{2t} \approx \left(\frac{u_i-v_j}{\sigma}\right)^2 \equiv e_i \\ r_i &= P\left(\chi_1^2 < e_i\right) \\ q_i &= \begin{cases} 0 & \text{if } r_i \le p_0, \\ \dfrac{r_i^a - p_0}{1-p_0} & \text{otherwise,} \end{cases} \\ \lambda_{(i)} &= \lambda_{\min} + (\lambda_{\max} - \lambda_{\min})\, q_i. \end{aligned}$$

Therefore, if we express (24) as

$$r_{jk} = \Pr\left\{Z_{jk}^L \le W_{t,j} \le Z_{jk}^U\right\},$$

where $W_{t,j} = (x_t - \nu_j)\,\lambda_t$, $Z_{jk}^L = \nu_k - \nu_j - \delta/2$ and $Z_{jk}^U = \nu_k - \nu_j + \delta/2$,; then $W_{t,j} = (x_t - \nu_j)\,\lambda_t \approx (u_i - \nu_j)\,\lambda_i \equiv w_i$ and it is possible to calculate r_{jk}. Finally, if $N = (\mathbf{I} - \mathbf{R})^{-1}\,\mathbf{u}$, we would calculate the ARL as

$$ARL = N\left((ms+1)/2\right).$$

For a given ARL_0 value, the following optimization nonlinear model with decision variables: $ARL\left(\delta\left(i\right) > 0, i = 1, 2, ..., k\right)$, $\lambda_{\min}, \lambda_{\max}, a, b, c, d, p_0$, and h, should be solved as

$$\begin{aligned} &\min f\left(ARL\left(\delta(i)\right)\right) \\ &\text{subject to:} \qquad\qquad , \\ &ARL\left(\delta = 0, \lambda_{\min}, \lambda_{\max}, a, p_0, h\right) = ARL_0 \end{aligned} \tag{25}$$

where $f\left(\cdot\right) : \mathbb{R}^n \to \mathbb{R}$, can be $\sum_{i=1}^{n}\left(ARL\left(\delta\left(i\right)\right)\right)$, the norm $\left\|ARL\left(\delta\left(i\right)\right)\right\|_2$, or some other convenient function. The $ARL\left(\delta\left(i\right), \cdots, h\right)$ is calculated using the Markov Chain procedure explained above using that $x_t \sim N(\mu_0 + \delta\sigma, \sigma^2)$. For simplicity, in the AEWMA2 and AEWMA3, the noncentral chi-squared distribution is replaced by the central chi-squared distribution because it has shown that both provide similar results.

Therefore, in a process control in zero state and $ARL_0 = 100$ with (13), and the optimality criteria: minimize the ARL at interval shifts $[0.5, 4]$ (AEWMA1-1, AEWMA2-1, AEWMA3-1) and at the interval shifts $[1, 4]$ (AEWMA1-2, AEWMA2-2, AEWMA3-2), Table 2 shows the optimal values of the AEWMA control chart parameters. Similarly, Table 3 shows the optimal values of parameters, for $ARL_0 = 500$. In this paper, for simplicity, and without loss of generality, the ARL values are computed assuming that $\mu_0 = 0$ and $\sigma = 1$. Tables 4 and 5 show the corresponding ARL profiles.

δ	AEWMA1-1	AEWMA2-1	AEWMA3-1	AEWMA1-2	AEWMA2-2	AEWMA3-2
$\lambda_{\min}$	0.0674	0.0653	0.0679	0.1629	0.1652	0.1643
$\lambda_{\max}$	0.1074	0.1264	0.1673	0.2521	0.2343	0.2274
a	188.3826	86.7717	322.0814	23.1215	68.5651	87.1643
p_0	0.7694	0.8289	0.5060	0.8701	0.3091	0.7382
h	0.3756	0.3696	0.3831	0.7024	0.7117	0.6975

Table 2: Optimal parameters of the AEWMA control chart designs. ARLo=100.

δ	AEWMA1-1	AEWMA2-1	AEWMA3-1	AEWMA1-2	AEWMA2-2	AEWMA3-2
$\lambda_{\min}$	0.0464	0.0242	0.0410	0.0141	0.1329	0.1308
$\lambda_{\max}$	0.1349	0.104	0.1428	0.1146	0.2266	0.1897
a	23.6780	8.5125	278.0239	0.4375	157.745	36.3608
p_0	0.9870	0.9978	0.8973	0.3303	0.7956	0.855
h	0.4059	0.2636	0.3745	0.7371	0.7791	0.7807

Table 3: Optimal parameters of the AEWMA control chart designs. ARLo=500.

δ	AEWMA1-1	AEWMA2-1	AEWMA3-1	AEWMA1-2	AEWMA2-2	AEWMA3-2
0.25	**40.55**	40.69	41.12	47.56	47.89	47.07
0.50	**17.56**	**17.65**	17.78	19.37	19.50	19.16
0.75	10.62	10.68	10.71	10.64	10.67	**10.55**
1.00	7.55	7.59	7.58	7.06	7.05	**7.03**
1.50	4.77	4.77	4.74	4.12	**4.10**	4.14
2.00	3.47	3.43	3.37	2.87	**2.85**	2.92
2.50	2.68	2.60	2.54	2.16	**2.15**	2.23
3.00	2.14	2.02	1.96	**1.69**	1.71	1.78
3.50	1.73	1.61	1.55	**1.39**	1.41	1.47
4.00	1.43	1.32	1.27	**1.19**	1.21	1.25
5.00	1.10	1.06	1.05	**1.03**	**1.03**	1.05

Table 4: The ARL values with ARLo=100.

δ	AEWMA1-1	AEWMA2-1	AEWMA3-1	AEWMA1-2	AEWMA2-2	AEWMA3-2
0.25	87.25	**78.40**	84.88	98.76	129.87	130.43
0.50	**29.64**	30.58	29.70	30.78	35.96	36.21
0.75	16.83	18.56	17.13	**16.42**	16.78	16.90
1.00	11.65	13.28	11.95	10.95	**10.39**	10.43
1.50	7.13	8.40	7.37	6.47	5.77	**5.75**
2.00	4.99	5.98	5.20	4.56	3.94	**3.91**
2.50	3.65	4.41	3.82	3.54	2.94	**2.92**
3.00	2.69	3.21	2.81	2.91	**2.26**	2.29
3.50	2.00	2.30	2.07	2.48	**1.78**	1.88
4.00	1.54	1.69	1.57	2.20	**1.44**	1.59
5.00	1.11	1.14	1.12	1.94	**1.09**	1.19

Table 5: The ARL values with ARLo=500.

4 Adaptive EWMA based on the value of the control statistics

In this AEWMA chart, denoted as AEWMA4, λ_t is based on the value of y_{t-1}. The statistics is proportional to the distance of y_{t-1} to the control limit $H = \mu_0 \pm h\sigma$, in consequence, the potential misadjustment is measured in base on the distance between y_{t-1} and the nearest control limit in a standardized measure on the interval $(0, 1)$. That distance is denote by D_t. The closer y_{t-1} is to the control limit, the closer D_t to 1 is. This is done by using the statistics

$$D_t = \left| \frac{y_{t-1} - \mu_0}{H - \mu_0} \right| = \left| \frac{y_{t-1} - \mu_0}{h\sigma} \right|,$$

that using (13) with $D_t = F_{1t}$ or (19) with $D_t = G_{2t}$, it can be translated to a time-varying smoothing parameter λ_t. Taking a specific design, Figure 5 shows that λ_t increases faster when the distance D_t increases. When the process is out of control, λ_t tends to take the greatest possible value.

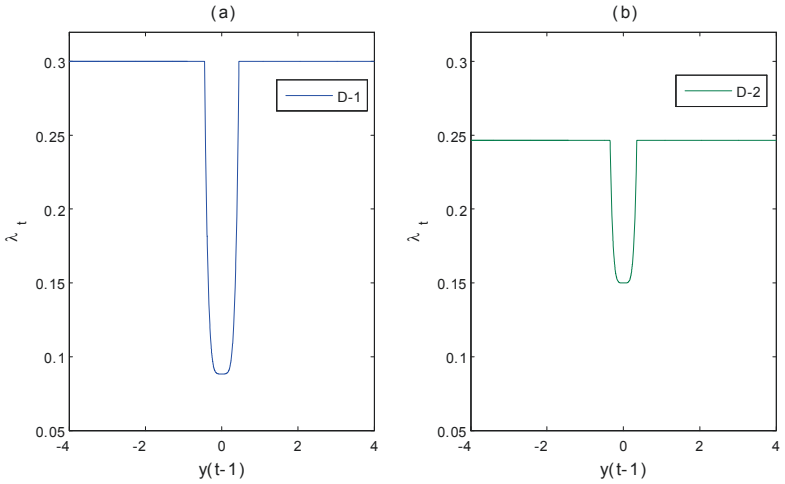

Figure 5: (a) Behavior of λ_t parameter in terms of x_t for a specific control chart design D-1. (b) Behavior of λ_t parameter in terms of behavior x_t for a specific AEMWA 2 control chart design D-2.

4.1 Computation of the ARL of the AEWMA4 using a Markov chain approach

In this AEWMA chart, since λ_t does not depend on x_t, it could follow the traditional procedure, i. e., taking (24)

$$\begin{aligned} r_{jk} &= \Pr\left\{\nu_k - \nu_j - \delta/2 \leq (x_t - \nu_j)\,\lambda_t \leq \nu_k - \nu_j + \delta/2\right\} \\ &= \Pr\left\{\frac{\nu_k - \nu_j - \delta/2}{\lambda_t} - \nu_j \leq x_t \leq \frac{\nu_k - \nu_j + \delta/2}{\lambda_t} - \nu_j\right\}, \end{aligned}$$

and then, if $N = (\mathbf{I} - \mathbf{R})^{-1}\,\mathbf{u}$, we would calculate the ARL as

$$ARL = N\left((ms + 1)/2\right).$$

δ	$ARL_0 = 100$		$ARL_0 = 500$	
	AEWMA4-1	**AEWMA4-2**	**AEWMA4-1**	**AEWMA4-2**
$\lambda_{\min}$	0.0882	0.2467	0.0284	0.0943
$\lambda_{\max}$	0.1382	1	0.7638	0.3034
a	10.0419	15.4316	3.364	9.9854
p_0	0.999	0.999	0.9988	0.7347
h	0.4515	0.9043	0.29	0.6212

Table 6: Optimal parameters of the AEWMA control chart designs.

δ	$ARL_0 = 100$		$ARL_0 = 500$	
	AEWMA4-1	**AEWMA4-2**	**AEWMA4-1**	**AEWMA4-2**
0.25	**40.87**	50.58	**78.38**	105.04
0.50	**17.43**	20.74	**29.00**	31.25
0.75	**10.36**	10.98	17.18	**15.94**
1.00	7.30	**7.05**	12.18	**10.42**
1.50	4.61	**3.99**	7.75	**6.15**
2.00	3.41	**2.82**	5.74	**4.41**
2.50	2.75	**2.22**	4.59	**3.48**
3.00	2.33	**1.85**	3.85	**2.91**
3.50	2.07	**1.58**	3.34	**2.51**
4.00	1.9	**1.37**	2.98	**2.21**
5.00	1.54	**1.09**	2.41	**1.96**

Table 7: The ARL values.

Applying (25), the optimal values of the parameters can be obtained. Therefore, in a process control in zero state and $ARL_0 = 100$ and 500, with optimality criteria: minimize the ARL at interval shifts $[0.5, 4]$ (AEWMA4-1) and at the interval shifts $[1, 4]$ (AEWMA4-2), the optimal values of parameters are shown in Table 6. The ARL profiles are shown in the Table 7.

5 Comparisons

In this section, the different AEWMA control charts and designs are compared. Also, they have been compared to other control charts like traditional EWMA control charts, Shewhart control chart, the AEWMA control charts of Capizzi and Masarotto (2003) and the ACUSUM of Jiang et al. (2008) control charts. Zero state ARL is considered and the ARL scale used in the figures is chosen to be logarithmic, unless otherwise stated.

For a specified in-control $ARL_0 = 100$, Figure 6-a shows that the performance of the four proposed AEWMA charts are similar for small shifts in the mean, in the range $\delta \in [0, 1.5]$, with AEWMA4-1 showing a slightly better performance. In the interval $1.5 < \delta < 5$, the first three AEWMA charts

show similar performance, being the third one slightly better than the others. It is possible to see the ARL of AEWMA3-1 is usually between ARL of AEWMA1-1 and AEWMA2-1. This behavior is expected since the third AEWMA chart is a combination of one and two AEWMA charts. The AEWMA4-1 loses efficiency for large shifts.

On the other hand, Figure 6-b shows that the four AEWMA performances also are similar for small shifts in the mean process, approximately $0 < \delta < 1.5$, again, for very small shifts AEWMA4-2 is slightly better than the others. In the interval $\delta \in [1.5, 5]$, the first three AEWMA charts show similar performance, being AEWMA3-1 slightly better than the others. It is possible to see that the ARL of AEWMA3-2 is usually between ARL of AEWMA1-2 and AEWMA2-2.

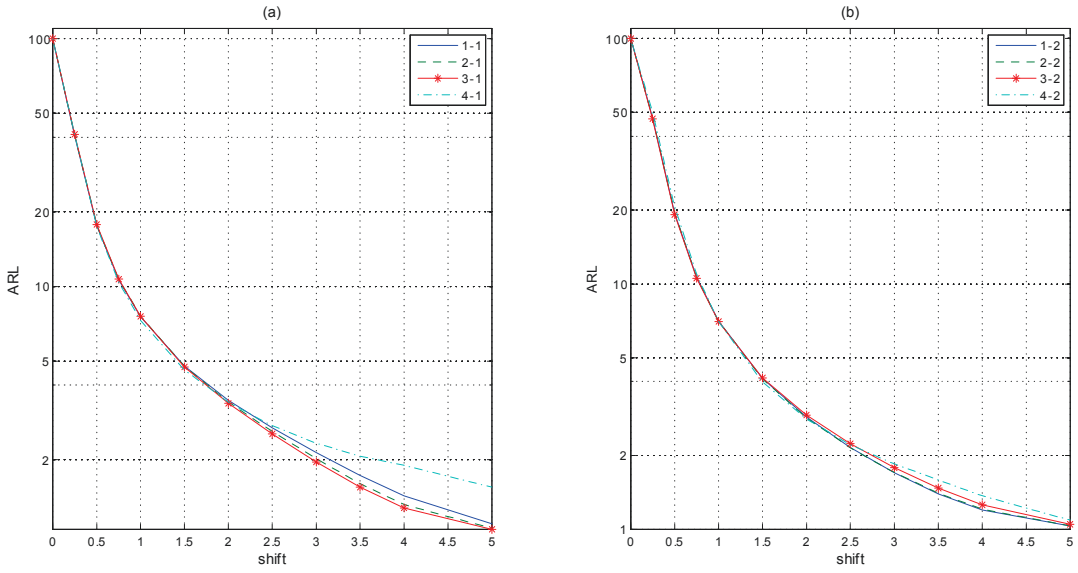

Figure 6: (a) ARL comparisons between the four AEWMA designs proposed, AEWMA-(1-1, 2-1, 3-1, 4-1: (—), (−−), (− ∗ −), (− · −)). (b) ARL comparisons between the four AEWMA designs proposed, AEWMA-(1-2, 2-2, 3-2, 4-2: (—), (−−), (− ∗ −), (− · −)). $ARL_0 = 100$.

For the case with $ARL_0 = 500$, Figure 7-a shows that the AEWMA4-1 is slightly the best for small shifts, approximately in the interval $0 < \delta < 1.5$. For large shifts, the AEWMA1-1 and 3-1 are very similar, and better than the others. Figure 7-b shows that for small shifts, in the interval $0 < \delta < 1$, all the charts are similar. For larger shifts, the AEWMA2-2 and 3-2 are the bests. In general, the four AEWMA charts show good behavior.

Figure 8-a compares the ARL values of the four AEWMA charts and three competing EWMA charts. An in-control $ARL_0 = 100$ is considered and the three EWMA charts were designed to get a minimum ARL values at shifts 0.5 (E-1), 3 (E-2) and 5 (E-3), respectively. In this case, it can be seen

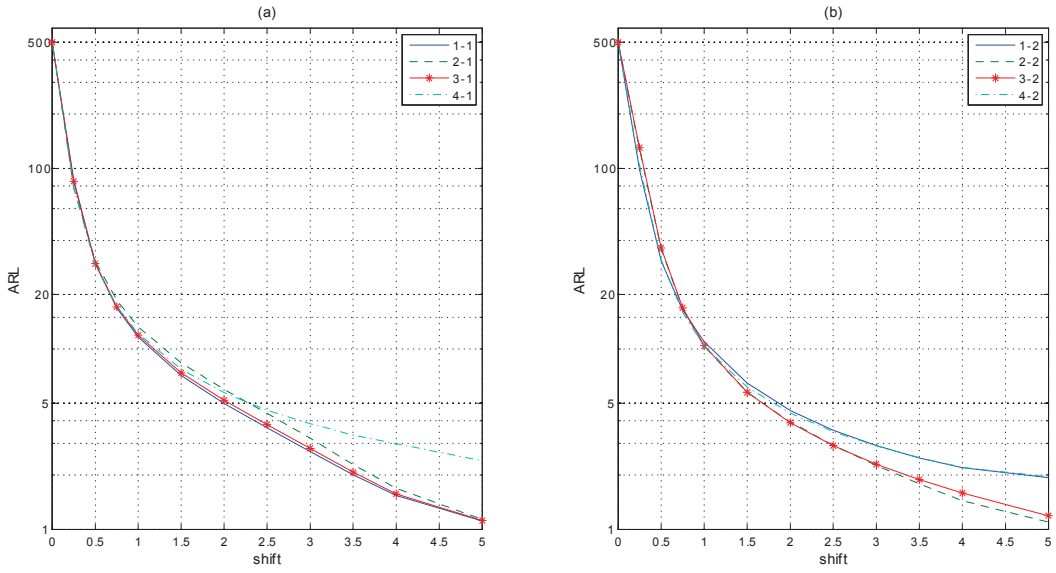

Figure 7: (a) ARL comparisons between 4 AEWMA designs proposed, AEWMA-(1-1, 2-1, 3-1, 4-1: (—), (−−), (−∗−), (−·−)). (b) ARL comparisons between 4 AEWMA designs proposed, AEWMA-(1-2, 2-2, 3-2, 4-2: (—), (−−), (− ∗ −), (− · −)). $ARL_0 = 500$.

that the four proposed AEWMA control charts and only the EWMA1 have a similar performance for small shifts, with AEWMA4-1 being slightly better than the others. For large shifts, approximately $\delta > 1.75$, the AEWMA charts are competitive with the EWMA2, EWMA3 control charts. Figure 8-b compares the ARL values of the four AEWMA charts (others four designs) and the same three EWMA charts. In this case, it can be seen that the four proposed AEWMA control charts and only EWMA1 have a competitive performance for small shifts, with AEWMA4-1 being slightly better than the others. For large shifts, approximately $\delta > 2$, the AEWMA charts are very competitive with the EWMA2, EWMA3 control charts.

For $ARL_0 = 500$, Figure 9 shows similar conclusions as in Figure (8). For $ARL_0 = 100$ and $ARL_0 = 500$, the Figure 10, and 11 respectively, compare the four AEWMA charts and a Shewhart control chart with rational subgroup size $n = 1$ (S-1). It can be seen that Shewhart control chart is not competitive for small shifts. Shewhart control chart is expected to be more efficient for large shifts. In general, the AEWMA1, 2 and 3 control charts are more competitive than Shewhart control chart in similar conditions, i. e. with $n = 1$.

Figures 12 compares the four proposed AEWMA control charts with two AEWMA designs of Capizzi and Masarotto (2003) based on the Huber score function. These two designs are considered by Capizzi and Masarotto (2003) as the best ones in terms of ARL (labelled as C&M-1and C&M-1).

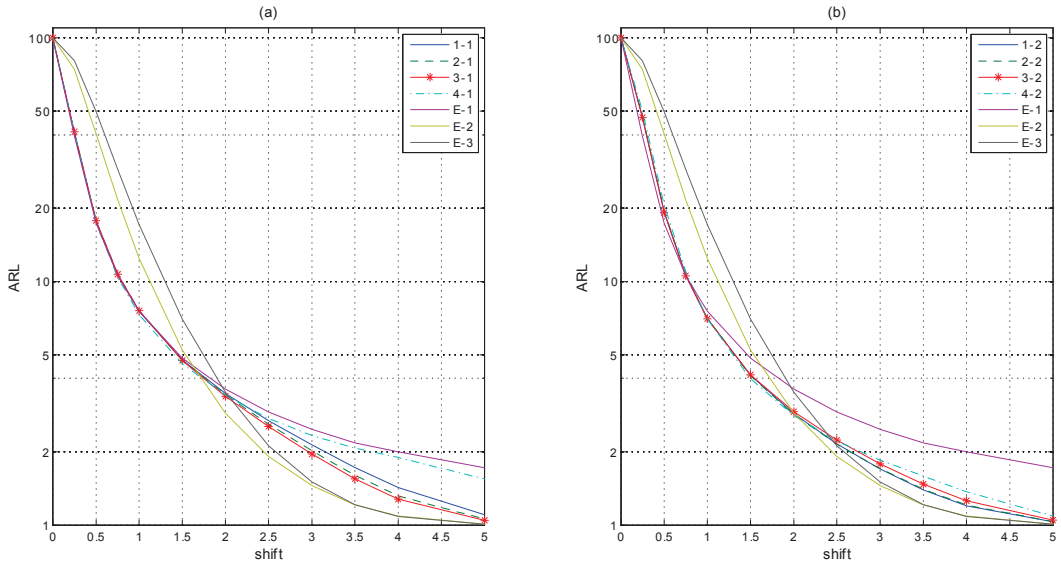

Figure 8: (a) ARL comparisons between 4 AEWMA designs proposed, AEWMA-(1-1, 2-1, 3-1, 4-1: (—), (−−), $(-*-)$, $(-\cdot-)$) and and EWMA (E-1, E-2, E-3: (—)). (b) ARL comparisons between 4 AEWMA designs proposed, AEWMA-(1-2, 2-2, 3-2, 4-2: (—), (−−), $(-*-)$, $(-\cdot-)$) and and EWMA (E-1, E-2, E-3: (—)). $ARL_0 = 100$.

It is assumed that $ARL_0 = 100$. It can be seen that the four proposed AEWMA charts and C&M-1 and 2 are very similar in almost all range of shifts. Figure 12-a shows that small differences occur in large shifts. It is interesting that AEWMA4-1 has a good performance for small changes but loses efficiency for large shift. Also, we can see that AEWMA3-1 is the most competitive control chart design for large shifts. For the small shifts, Figure 12-a shows similar control chart performances. For large shifts, The AEWMA1-2 and 2-2 are the most competitive control charts. In general, the control charts proposed are very competitive.

With $ARL_0 = 500$, Figure 13 shows the comparisons of the same control charts. It can be seen that the proposed AEWMA charts are very competitive for small shifts, specifically the AEWMA1 and AEWMA4. Figure 13-a shows the AEWMA1-1, 3-1 and C&M-1 are the most competitive control charts. For large shifts, Figure 13-b shows the C&M-2 is the most competitive control chart, however, AEWMA1-2 and 2-2 present a very good performance.

Our final comparison is between the proposed AEWMA control chats and two ACUSUM charts of Jiang et al. (2008) (see Figure 14). For $ARL_0 = 500$, the ACUSUM charts were optimized for detecting mean shifts over the range $[0.5, 4]$ (ACUSUM J-1) and $[1, 5]$ (ACUSUM J-2), respectively. It can be seen that the proposed AEWMA charts are very competitive for small shifts, specifically

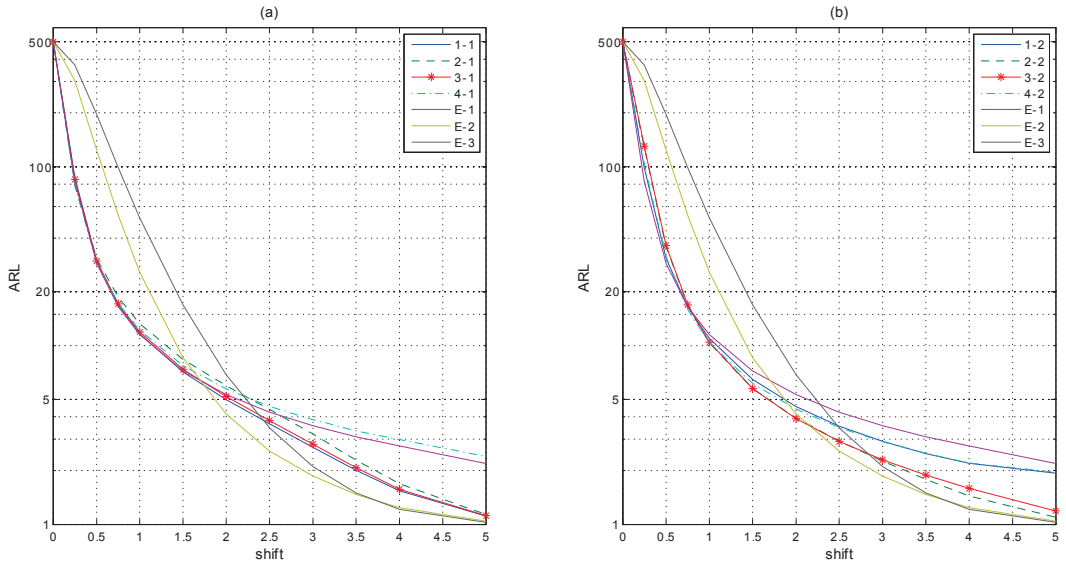

Figure 9: (a) ARL comparisons between 4 AEWMA designs proposed, AEWMA-(1-1, 2-1, 3-1, 4-1: (—), (−−), (− ∗ −), (− · −)) and EWMA (E-1, E-2, E-3: (—)). (b) ARL comparisons between 4 AEWMA designs proposed, AEWMA-(1-2, 2-2, 3-2, 4-2: (—), (−−), (− ∗ −), (− · −)) and EWMA (E-1, E-2, E-3: (—)). $ARL_0 = 500$.

the AEWMA3-1 and 4-1 are the most competitive control charts. For large shifts, Figure 14-a shows AEWMA1-1, 3-1 and ACUSUM J-1 are very competitive control charts. On the other hand, for large shift, Figure 14-b shows that AEWMA2-2 and 3-2 have a good performance. Tables 8 and 9 summarize the ARL values of the different control charts considered in this comparisons for $ARL_0 = 100$ and $ARL_0 = 500$ respectively.

6 Conclusions

We have presented four adaptive control charts for monitoring the mean of a variable that represents a quality characteristic in a particular process. These control charts work with a time varying smoothing parameter. The proposed AEWMA charts are very easy to understand and implement in practice. We should have in mind that the size shift depends on the nature of the monitored process. Since in actual operation, smaller shifts are more frequent than larger shifts, we have prioritized the study for small and medium shifts. However, the proposed charts can be competitive with respect to alternative charts in the literature on a wide range of shifts.

δ	**E-1,** λ**= 0.05**	**E-2,** λ**= 0.3**	**E-3,** λ**= 0.5**	**S-1,** $(\mathbf{n = 1})$	**C&M-1**	**C&M-2**
0.25	**39.61**	74.17	80.62	80.83	40.08	47.81
0.50	**17.33**	40.29	49.65	49.99	17.52	19.53
0.75	**10.56**	21.62	28.80	29.09	10.63	10.63
1.00	7.55	12.44	17.13	17.33	7.56	**7.00**
1.50	4.85	5.24	7.01	7.09	4.78	**4.09**
2.00	3.61	**2.88**	3.51	3.54	3.46	2.89
2.50	2.92	**1.92**	2.12	2.13	2.64	2.23
3.00	2.47	**1.45**	1.50	1.51	2.05	1.80
3.50	2.18	**1.21**	1.22	1.22	1.62	1.51
4.00	1.99	1.09	**1.08**	**1.08**	1.32	1.29
5.00	1.72	**1.01**	**1.01**	**1.01**	1.06	1.06

Table 8: The ARL values with ARLo=100.

δ	**E-1,** λ**= 0.05**	**E-2,** λ**= 0.3**	**E-3,** λ**= 0.5**	**S-1,**$(\mathbf{n = 1})$	**C&M-1**	**C&M-2**	**J-1**	**J-2**
0.25	**82.76**	302.88	369.86	374.17	86.41	130.87	96.34	147.49
0.50	**28.76**	123.94	195.74	201.58	29.91	36.38	31.47	39.25
0.75	**16.50**	53.34	98.82	103.12	17.11	16.94	17.66	17.42
1.00	11.52	25.82	51.85	54.59	11.88	**10.45**	12.18	10.57
1.50	7.23	8.57	16.88	17.89	7.27	**5.78**	7.40	5.81
2.00	5.32	4.15	6.88	7.26	5.06	**3.95**	5.15	3.99
2.50	4.24	**2.58**	3.47	3.60	3.65	2.94	3.75	3.00
3.00	3.56	**1.86**	2.11	2.15	2.64	2.26	2.79	2.37
3.50	3.10	**1.48**	1.50	1.52	1.92	1.76	2.12	1.91
4.00	2.75	1.24	1.22	**1.22**	1.47	1.42	1.67	1.57
5.00	2.19	1.04	**1.03**	**1.03**	1.08	1.08	1.18	1.17

Table 9: The ARL values with ARLo=500.

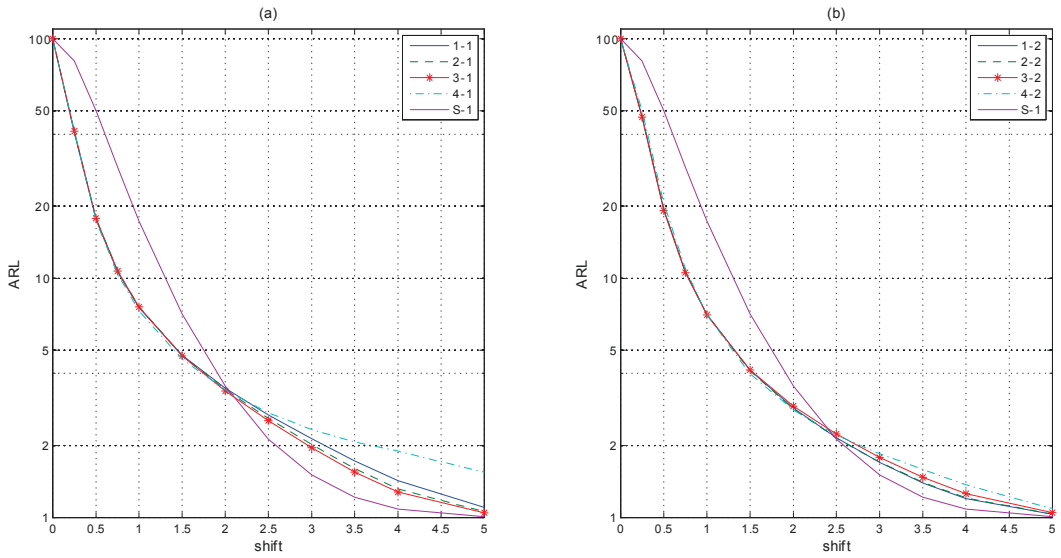

Figure 10: (a) ARL comparisons between 4 AEWMA designs proposed, AEWMA-(1-1, 2-1, 3-1, 4-1: (—), (−−), $(-*-)$, $(-\cdot-)$) and Shewhart $n = 1$ and $n = 3$ (S-1, S-2: (—)). (b) ARL comparisons between 4 AEWMA designs proposed, AEWMA-(1-2, 2-2, 3-2, 4-2: (—), (−−), $(-*-)$, $(-\cdot-)$) and Shewhart $n = 1$ and $n = 3$ (S-1, S-2: (—)). $ARL_0 = 100$.

6.0.1 Acknowledgements

The authors would like to thank Dr. Andrés M. Alonso for his useful comments on previous versions of the manuscript. The authors also gratefully acknowledge the financial support received from the Spanish MEC, under grant ECO2012-38442.

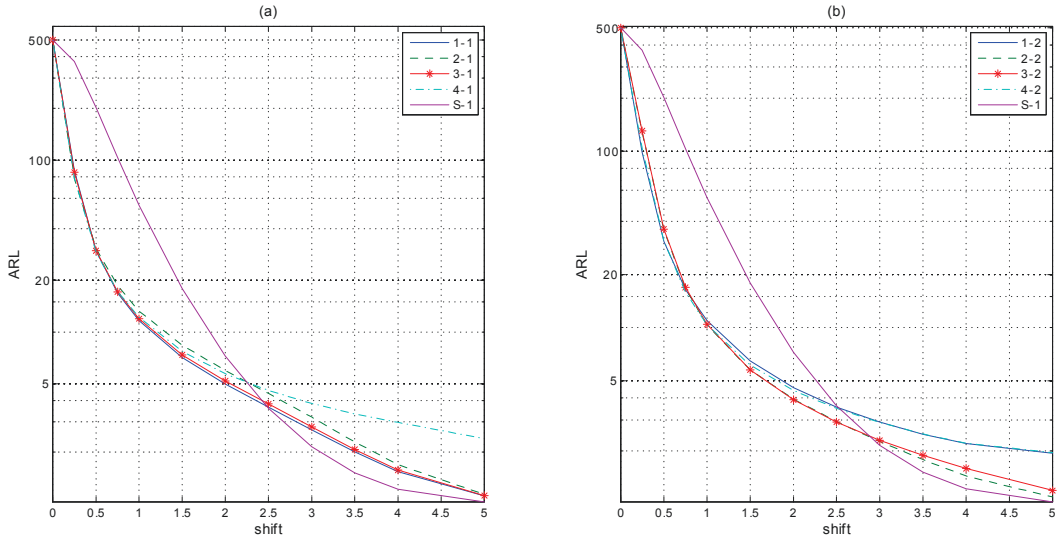

Figure 11: (a) ARL comparisons between 4 AEWMA designs proposed, AEWMA-(1-1, 2-1, 3-1, 4-1: (—), (−−), (− ∗ −), (− · −)) and Shewhart $n = 1$ and $n = 3$ (S-1, S-2: (—)). (b) ARL comparisons between 4 AEWMA designs proposed, AEWMA-(1-2, 2-2, 3-2, 4-2: (—), (−−), (− ∗ −), (− · −)) and Shewhart $n = 1$ and $n = 3$ (S-1, S-2: (—)). $ARL_0 = 500$.

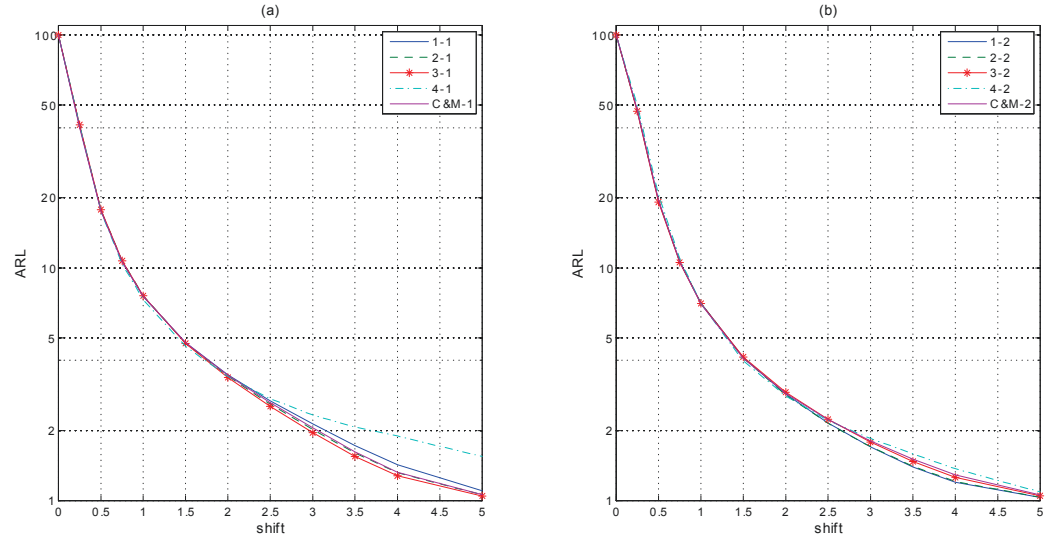

Figure 12: (a) ARL comparisons between 4 AEWMA designs proposed and AEWMA C&M-1 (—). (b) ARL comparisons between 4 AEWMA designs proposed and AEWMA C&M-2 (—). For $ARL_0 = 100$.

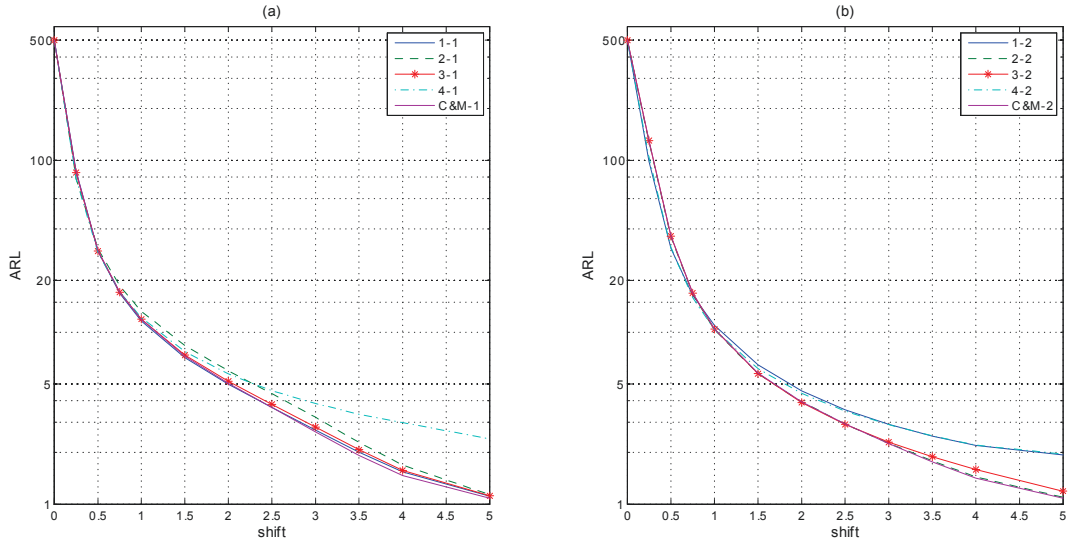

Figure 13: (a) ARL comparisons between 4 AEWMA designs proposed and AEWMA C&M-1 (—). (b) ARL comparisons between 4 AEWMA designs proposed and AEWMA C&M-2 (—). For $ARL_0 = 500$.

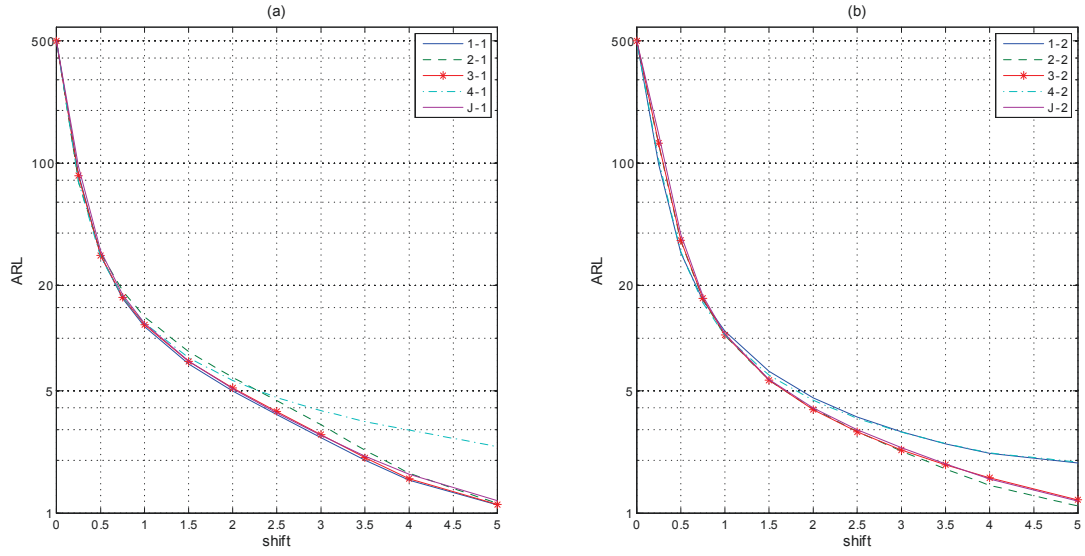

Figure 14: (a) ARL comparisons between 4 AEWMA designs proposed, ACUSUM J-1 (—). (b) ARL comparisons between 4 AEWMA designs proposed, ACUSUM J-2 (—). $ARL_0 = 500$.

References

[1] Acosta-Mejia C. A. (2007). Two sets of runs rules for the $\bar{X}$ chart. Quality Engineering, 19, pp. 129-136.

[2] Antzoulakos D. L. and Rakitzis A. C. (2008). The revised m-of-k runs rule. Quality Engineering, 20(1), pp. 75-81.

[3] Arnold, J. C.and Reynolds, M. R. (2001). CUSUM control charts with variable sample sizes and sampling intervals. Journal of Quality Technology, 33(1), 66-81.

[4] Baxley R. V. (1995). An application of variable sampling interval control chart. Journal of Quality Technology, 27, pp. 275–282.

[5] Beaton A. E. and Tukey J. W. (1974). The fitting of power series, meaning polynomials, illustrated on Band-Spectroscopie data. Technometrics, 16, pp. 147-185.

[6] Capizzi G. and Masarotto G. (2003). An adaptive exponentially weighted moving average control chart. Technometrics, 45, pp. 199-207.

[7] Castagliola, P., Zhang, Y., Costa, A., and Maravelakis, P. (2012). The variable sample size $\bar{X}$ chart with estimated parameters. Quality and Reliability Engineering International, 28(7), 687-699.

[8] Champ C. W. and Woodall W. H. (1987). Exact results for Shewhart control charts with supplementary runs rules. Technometrics, 29, pp. 393-399.

[9] Costa A. F. (1994). $\bar{X}$ charts with variable sample size. Journal of Quality Technology, 26(3), pp. 155-163.

[10] Costa A. F. B. (1999a). Joint $\bar{X}$ and R charts with variable sample sizes and sampling intervals. Journal of Quality Technology, 31(4), pp. 387-397.

[11] Costa A. F. (1999b). $\bar{X}$ charts with variable parameters. Journal of Quality Technology, 31, pp. 408-416.

[12] Costa A. F. B. and Rahim M. A. (2006). A single EWMA chart for monitoring process mean and process variance. Quality Technology & Quantitative Management, 3, pp. 295-305.

[13] Crowder S. V. (1987a). Average run lengths of exponentially weighted moving average control charts. Journal of Quality Technology, 19, pp. 161-164.

[14] Crowder S. V. (1989). Design of exponentially weighted moving average schemes. Journal of Quality Technology, 21(3), pp. 155-162.

[15] Cui R. Q. and Reynolds M. R. (1988). Chart with runs and variable sampling intervals. Communications in Statistics-Simulation and Computation, 17(3), pp. 1073-1093.

[16] Daudin J. J. (1992). Double sampling $\bar{X}$ charts. Journal of Quality Technology, Vol. 24(2), pp.78-87.

[17] Davis R. B. and Woodall W. H. (1988). Performance of the control chart trend rule under linear shift. Journal of Quality Technology, 20(4), pp. 260-262.

[18] Davis R. B., Homer A. and Woodall W. H. (1990). Performance of the zone control chart. Communications in Statistics-Theory and Methods, 19(5), pp. 1581-1587.

[19] Derman C. and Ross S. M. (1997). Statistical aspects of quality control. San Diego, CA: Academic Press.

[20] Han D. and Tsung F. (2004). A generalized EWMA control chart and its comparison with the optimal EWMA, CUSUM and GLR schemes. The Annals of Statistics, 32(1), 316-339.

[21] Han D., Tsung F. and Li Y. (2007). A CUSUM chart with local signal amplification for detecting a range of unknown shifts. International Journal of Reliability, Quality and Safety Engineering, 14(02), pp. 81-97.

[22] Hawkins D. M. (1992). A fast, accurate approximation of average run lengths of CUSUM control charts. Journal of Quality Technology, 24(1), pp. 37-43.

[23] Hawkins D. M. (1993). Cumulative sum control charting: An underutilized SPC tool. Quality Engineering, 5(3), 463-477.

[24] Huber P. J. (1981). Robust statistics. New York: Wiley.

[25] Hunter J. S. (1986). The exponentially weighted moving average. Journal of Quality Technology 18, pp. 203-210.

[26] Jiang W., Shu L. and Apley D. W. (2008). Adaptive CUSUM procedures with EWMA-based shift estimators. IIE Transactions, 40, pp. 992-1003.

[27] Keats J. B., Miskulin J. D. and Runger G. C. (1995). Statistical process control scheme design. Journal of Quality Technology, 27(3), pp. 214-225.

[28] Khoo M. B. C. and Ariffin K. N. B. (2006). Two improved runs rules for the Shewhart control chart. Quality Engineering, 18(2), pp. 173-178.

[29] Klein M. (2000). Two alternatives to the Shewhart $\bar{X}$ control chart. Journal of Quality Technology, 32(4), pp. 427-431.

[30] Koutras M. V., Bersimis S. and Maravelakis P. E. (2007). Statistical process control using Shewhart control charts with supplementary runs rules. Methodology and Computing in Applied Probability, 9, pp. 207-224

[31] Lucas J. M. and Saccucci M. S. (1990). Exponentially weighted moving average control schemes: Properties and Enhancements (with discussion), Technometrics, 32(1), pp. 1-29.

[32] Mahadik S. B. (2013). $\bar{X}$ Charts with variable sample size, sampling interval, and warning limits. Quality and Reliability Engineering International, 29(4), pp. 535–544.

[33] Montgomery D. C., Gardiner J. S. and Pizzano B. A. (1987). Statistical process control methods for detecting small process shifts. In Frontiers in Statistical Quality Control, eds. H.-J. Lenz, G. B. Wetherill, and P. T. Wilrich, Heidelberg, West Germany: Physica-Verlag, pp. 161-178.

[34] Nelson C. S. (1984). The Shewhart control charts - test for special causes. Journal of Quality Technology, 16, pp. 237-239.

[35] Page E. S. (1954). Continuous inspection schemes. Biometrika, 41, pp. 100 – 114.

[36] Page E. S. (1955a). Control charts with warning lines. Biometrika, 42(1-2), pp. 243-257.

[37] Page E. S. (1955b). A test for a change in a parameter occurring at an unknown point. Biometrika, 42, pp. 523-527.

[38] Prabhu S. S., Runger G. C. and Keats J. B. (1993). $\bar{X}$ chart with adaptive sample sizes. The International Journal of Production Research, 31(12), pp. 2895-2909.

[39] Prabhu S. S., Montgomery D. C. and Runger G. C. (1994). A combined adaptive sample size and sampling interval $\bar{X}$ control scheme. Journal of Quality Technology, 26(3), pp. 164-176.

[40] Reynolds J. H. (1971). The run sum control chart procedure. Journal of Quality Technology, 3(1), pp. 23-27.

[41] Reynolds M. R. (1995). Evaluating properties of variable sampling interval control charts. Sequential Analysis, 14(1), pp. 59-97.

[42] Reynolds M. R. (1996a). Shewhart and EWMA variable sampling interval control charts with sampling at fixed times. Journal of Quality Tecnology, 28, pp. 199-212.

[43] Reynolds M. R. (1996b). Variable-sampling-interval control charts with sampling at fixed times. IIE transactions, 28(6), pp. 497-510.

[44] Reynolds, M. R., and Arnold, J. C. (2001). EWMA control charts with variable sample sizes and variable sampling intervals. IIE transactions, 33(6), 511-530.

[45] Reynolds, M. R., and Stoumbos, Z. G. (1998). The SPRT chart for monitoring a proportion. IIE transactions, 30(6), 545-561.

[46] Reynolds M. R, Amin R. W., Arnold J. C. and Nachlas J. A. (1988). $\bar{X}$ Charts with Variable Sampling Intervals. Technometrics, 30(2), pp. 181-192.

[47] Reynolds M. R., Amin R. W. and Arnold J. C. (1990). CUSUM charts with variable sampling intervals. Technometrics, 32(4), pp. 371-384.

[48] Roberts S. W. (1959). Control chart tests based on geometric moving averages. Technometrics, 1(3), pp. 239-250.

[49] Robinson P. B. and Ho T. Y. (1978). Average run lengths of geometric moving averages by numerical methods. Technometrics, 20(1), pp. 85-93.

[50] Runger G. C. and Pignatiello J. J. (1991). Adaptive sampling for process control. Journal of Quality Technology, 23(2), pp. 135-155.

[51] Sawalapurkar-Powers U., Arnold J. C. and Reynolds M. R. (1990). Variable sample size control charts. In the Annual Meeting of the American Statistical Association, Orlando, FL.

[52] Shewhart W. A. (1931). Economic control of quality of manufactured product. D. Van Nostrand Company, Inc, The United States of America, pp. 182.

[53] Shu L. (2008). An adaptive exponentially weighted moving average control chart for monitoring process variances. Journal of Statistical Computation and Simulation, 78(4), pp. 367-384.

[54] Shu L. and Jiang W. (2006). A Markov chain model for the adaptive CUSUM control chart. Journal of Quality Technology, 38, pp. 135-147.

[55] Shu L., Jiang W. and Wu Z. (2008). Adaptive CUSUM procedures with Markovian mean estimation. Computational Statistics & Data Analysis, 52(9), pp. 4395-4409.

[56] Sparks R. (2000). CUSUM charts for signaling varying location shifts. Journal of Quality Technology, 32, pp. 157-171.

[57] Steiner S. H. (1999). Exponentially weighted moving average control charts with time varying control limits and fast initial response. Journal of Quality Technology, 31(0), pp. 75-86.

[58] Stoumbos Z. G. and Reynolds M. R. (1996). Control charts applying a general sequential test at each sampling point. Sequential Analysis, 15(2-3), pp. 159-183.

[59] Stoumbos Z. G. and Reynolds M. R. (1997). Corrected diffusion theory approximations in evaluating properties of SPRT charts for monitoring a process mean. Proceedings of the 2nd World Congress of Nonlinear Analysts, 30(7), pp. 3987-3996.

[60] Tagaras G. (1998). A survey of recent developments in the design of adaptive control charts. Journal of Quality Technology, 30(3), pp. 212-231.

[61] Vance L. C. (1986). Average run lengths of cumulative sum control charts for controlling normal means. Journal of Quality Technology, 18, pp. 189-193.

[62] Waldmann K. H. (1986). Bounds for the distribution of the run length of geometric moving average charts. J. R. Star. Soc., Set. C, Appl. Stat. 35, pp. 151-158.

[63] Western Electric (1956). Statistical quality control handbook. Western Electric Corporation, Indianapolis, Ind.

[64] Woodall W. H. and Adams B. M. (1993). The statistical design of CUSUM charts. Quality Engineering, 5, pp. 559-570.

[65] Yashchin, E. (1987). Some aspects of the theory of statistical control schemes. IBM Journal of Research and Development, 31(2), 199-205.

[66] Wu, S. (2011). Optimal inspection policy for three-state systems monitored by variable sample size control charts. The International Journal of Advanced Manufacturing Technology, 55(5-8), 689-697.

[67] Zhang, J., Li, Z., and Wang, Z. (2012). A new adaptive control chart for monitoring process mean and variability. The International Journal of Advanced Manufacturing Technology, 60(9-12), 1031-1038.

[68] Zimmer L.S., Montgomery D.C and Runger G.C. (1998). Evaluation of a three-state adaptive sample size $\bar{X}$ control chart. International Journal of Production Research, 36(3), pp. 733-743.